Atmospheric In-cloud Icing Using WRF for an Alpine Wind Power Plant in Norway

Jonas Mundheim Strand[1,2], Yngve Birkelund[1], Pravin Punde[1]

[1] *University of Tromsø - The Arctic University of Norway*
[2] *Kjeller Vindteknikk (part of Norconsult), Norway*

Jonas.mundheim.strand@norconsult.com, yngve.birkelund@uit.no, pravin.b.punde@uit.no,

***Abstract*— Troms Kraft have identified a location in Kvænangen, Norway, for a new wind power plant with promising wind resources. However, the site is in an arctic climate with mountainous terrain exposed to severe icing conditions.**

Assessments of icing conditions at proposed locations for new wind power plants in areas exposed to icing is crucial to identifying icing related challenges. This paper investigates atmospheric in-cloud icing and thereby identifying conditions affecting the wind turbines at the proposed site. Meteorological parameters are provided from simulations using the Weather Research and Forecasting (WRF) model. Modelled parameters are applied to calculate estimates of the expected annual hours with ice accretion rate exceeding threshold values 10 g/h and 50 g/h for suggested turbine locations. This is done by applying the Makkonen ice accretion model. The WRF model has been run for the whole of 2022.

It is found that model terrain elevation is strongly connected to the calculated ice accretion rate. Because of this, a method for adjusting the icing estimations to differences between model and actual terrain height is conducted.

Analysis of wind patterns at times with modelled meteorological icing shows that ice accretion normally accumulates during winds coming from north-westerly directions. Case studies shows that icing conditions with north-westerly winds induce an increased LWC as a result of orographic lifting.

Keywords— ***In-cloud icing, WRF, Orographic lifting, Norway, Wind power, Arctic***

I. Introduction

Wind power production in arctic regions face significant challenges related to atmospheric icing. Accumulation of ice, most frequently caused by in-cloud icing, on structures like turbine blades and power lines can result in severe damage. Ice accretion on turbine blades can adversely impact the aerodynamics of the blade and reduce the turbines production [1]. A combination of imbalances in ice mass and aerodynamics may cause vibrations increasing the risk of mechanical failure [2]. Accumulation of ice on the turbines may exert serious safety hazards for people and infrastructure in case of ice shedding [3].

Early assessments of the icing conditions at specific locations becomes increasingly important as a part of the developing process of a new wind power plant. In the search for great wind resources energy companies look to construct in mountainous areas. This also results in an increased exposure to severe icing which will affect both power production and maintenance costs [4][5][6].

Detailed information regarding the icing conditions can be utilized to compare estimated production loss due to icing between prospected sites. This can prove to be essential when assessing turbine placements and evaluate locations for construction. Local meteorological patterns found from conditional analysis could be useful for forecasting icing events [7].

II. Method

A. Data

The site of interest in this paper is located south of Kvænangsbotn, in Kvænangen municipality, Troms County. The suggested wind turbines are located in mountainous terrain with topography varying from 700 – 900 meters above sea level surrounded by complex terrain in all directions. The site is placed at the top of a steep terrain elevation from Sørfjorden (0 masl) to the north of the site, meaning all winds blowing from N-NW directions will be orographically lifted before reaching the site. In south/south-east and easterly directions the terrain can be described as relatively flat and in-land climate. Low pressure systems typically bring precipitation from the ocean during winter season, while easterly wind is cold and dry.

All data in this study is retrieved from simulation done by Weather Research and Forecasting model, version 4.3. WRF is a three-dimensional, fully compressible, nonhydrostatic state of the art numerical weather prediction model designed for different mesoscale applications. The model is developed by National Centre of Atmospheric Research (NCAR) and is used for both research and forecast purposes [8].

The WRF model has been run for the whole of 2022 with three one-way nesting domains d01, d02 and d03 with grid spacing 9km, 3km and 1km (Fig. 1). All domains are configured with a vertical structure of 51 terrain following sigma levels with 50 hPa as upper boundary layer. The simulation is initiated and forced on the lateral boundaries by the ECMWF-ERA5 dataset [9]. Global Multi-resolution Terrain Elevation Data 2010 (GMTED 2010) with horizontal resolution 30 arc-seconds (1km) is used as terrain input data. Parameterization schemes used are listed in Table I.

TABLE I. PARAMETERIZATION SCHEMES USED IN THE WRF SIMULATION

Type of scheme	WRF variable name	Scheme
Microphysics	mp_physics	Thompson [10]
Planetary boundary	bl_pbl_physics	YSU [11]
Shortwave radiation	ra_sw_physics	RRTMG [12]
Longwave radiation	ra_lw_physics	RRTMG [12]
Land surface	sf_surface_physics	Unified Noah [13]

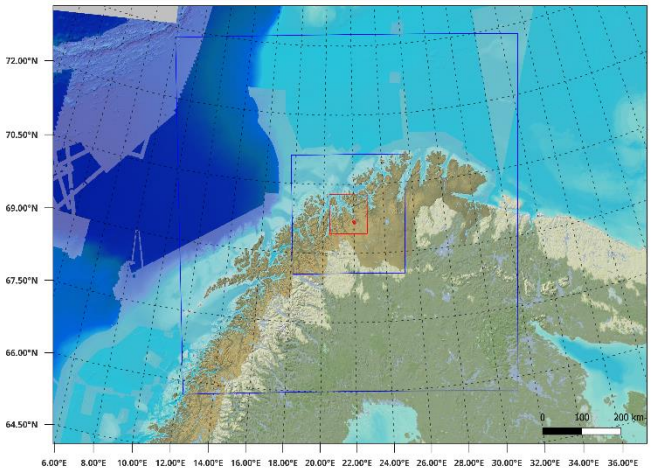

Fig. 1 Domain configuration of nested domains used in the WRF simulation. d01 (outer square), d02 (middle square) and d03 (inner red square). The site of interest is marked in red within d03.

B. *Theoretical calculations*

The ice accretion rate is calculated using the output data from WRF-d03 as input in the Makkonen model described in [14] on a standard reference collector (SRC) with dimensions 30mm diameter and 1m length. This follows the equation

$$\frac{dM}{dt} = \alpha_1 \alpha_2 \alpha_3 v A (LWC)$$

The accreted ice mass (dM/dt) [kg/s], is a function of the collision efficiency, α_1, the sticking efficiency (mainly for wet snow), α_2, the freezing efficiency (determines "dry and "wet" growth for rime), α_3 , the wind speed (perpendicular to accreting object), v [m/s] , the cross-sectional area of object, A [m^2], and the liquid water content, LWC [kg/m^3]. All the terms α_1, α_2 and α_3 are correction factors with a value in the range 0 to 1.

In this study $\alpha_1 = \alpha_2 = 1$ giving an assumption of dry ice growth, hence all impinging droplets will freeze on impact with the SRC. α_1 and MVD is calculated from the following equations [15]

$$MVD = \frac{(3.672 + \mu)}{\lambda}$$

Where μ is the shape parameter, diagnosed by the pre-specified droplet concentration number, N_c [m^{-3}]. $N_c = 100$ cm^{-3} is used in the calculations for this paper.

$$\mu = \min\left(\frac{1000}{N_c} + 2,15\right)$$

And λ is found using gamma distribution, with ρ_w as the density of water [kg/m^3]

$$\lambda = \left[\frac{\pi}{6}\rho_w \left(\frac{\Gamma(4+\mu)}{\Gamma(1+\mu)}\right)\left(\frac{N_c}{LWC}\right)\right]^{\frac{1}{3}}$$

The MVD can then be used to calculate the collision efficiency from

$$\alpha_1 = A - 0.028 - C(B - 0.0454)$$

Where

$$A = 1.066K^{-0.00616}\exp(-1.103K^{-0.688})$$

$$B = 3.641K^{-0.498}\exp(-1.497K^{-0.694})$$

$$C = 0.00637(\phi - 100)^{0.381}$$

And the dimensionless parameters, droplet inertia parameter, K, and Langmuir parameter, ϕ

$$K = \frac{\rho_w MVD^2 v}{9uD}$$

$$\phi = \frac{Re^2}{K}$$

$$Re = \frac{\rho_a MVD v}{u}$$

Where D is the diameter of the cylinder and Re is the Reynolds number given by air density, ρ_a [kg/m^3], dynamic viscosity of air, u [$kg/m\ s$] and the free stream velocity, v [m/s].

Icing intensity, I [g/h], is then used to calculate annual hours with hourly average ice accretion rate exceeding a threshold value of 10 g/h, known as the industry limit [16]. Moreover, atmospheric in-cloud icing occurs for temperatures less than 0 °C. Therefore, only hourly average values with a threshold value of $T < 0$°C are included.

It is found that model terrain elevation is strongly connected to the calculated ice accretion rate. Because of this, a method for adjusting the icing estimations to differences between model and actual terrain height is conducted. This method is described in [17].

III. Results

A. *WRF model terrain height*

A closer look at the WRF-d03 models' terrain representation is depicted in Fig. 2. Limitations regarding representation of the terrain in the model will affect the output data at the site, and the influence of terrain and especially local terrain features as nearby mountains in westerly directions is not accurately represented which is important when describing the icing potential. This misrepresentation of steep elevation changes and actual elevation, in combination with the wind direction of the site, may influence the model icing results. The magnitude of this relation in the represented case will remain unknow as no actual observations at the site is available for comparison.

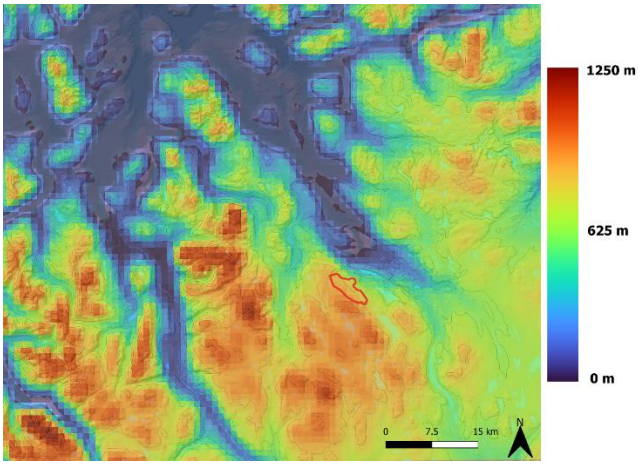

Fig. 2 Terrain height for WRF model domain - d03.

B. *Icing conditions analysis*

A wind rose representing wind directions and wind speeds during hours when icing intensity exceeds 10 g/h for a suggested turbine location within the site is shown in Fig. 3.

The results show that ice accretion mainly forms with winds blowing from NW directions for both threshold values. This is a strong indication of winds following the fjord resulting in orographically lifting of air before reaching the site. Due to the location characteristics at the top of a hill, the site is likely for NW winds to experience a much higher LWC than surrounding areas. This effect will intensify the icing at the site.

C. *Icing event*

Through investigations of hourly averaged ice accretion rate for the whole of 2022 we can identify icing events. This paper will further inspect an event in January characterized by winds blowing from north-west which is the direction most common for ice accretion at the site.

Fig. 4 shows a timeseries plot for the hourly averaged values for ice accretion rate, temperature, wind speed and MVD during an icing event starting at hour 03:00 on the 20th

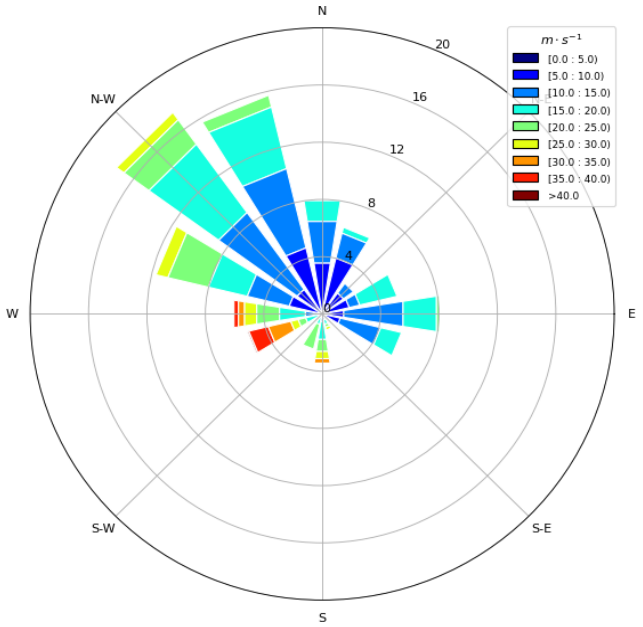

Fig. 3 Wind rose during times when icing intensity exceeds 10 g/h at height 174 m.a.s.

and ending 00:00 in the 21st. Throughout the event we identify a sustained icing event marked by large fluctuations in the estimated icing intensity. The temperature is well below freezing for the whole period and incidents with no-icing cannot be explained by positive temperatures in the model.

Investigating the results, we find increasing ice accretion rate with higher values for MVD and wind speeds. As expected, there is a prominent relation to warmer temperatures and high MVD, however, for the specific case at time 20:00 (20.01) we can observe an interesting high MVD during lower temperatures. The cause of this spike in MVD is not investigated but a relation between MVD and wind speeds seems to be present. This could be a result of increased terrain-induced vertical atmospheric-motions as the main forcing for production of LWC for higher wind speeds.

Usually, temperatures this low seem to inflict less icing than depicted in the graphical representation. Inspecting characteristics in the air masses before reaching the turbine could help explain this.

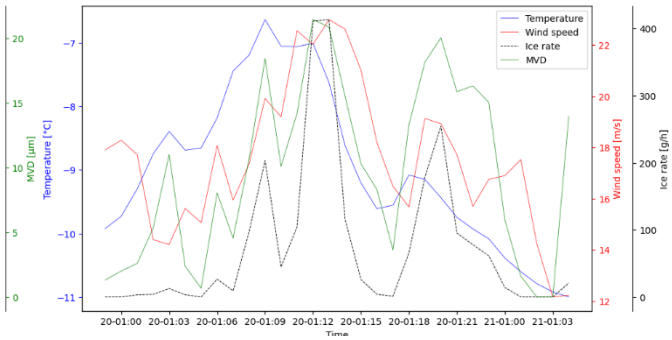

Fig. 4 Timeseries for period from 00:00 at the 20.01.2022 to 04:00 at the 21.01.2022. Hourly averaged values at height 174 m.a.s. for; ice accretion rate (dashed line), temperature (blue), MVD (green) and wind speed (red).

Fig. 5 displays a wind rose showing the direction of the wind during meteorological icing for the period 20th to 21st. This clearly shows a main direction of winds blowing from north-westerly directions, which is the same direction as the yearly overall main direction during ice accretion (Fig. 3).

Fig. 6 shows LWC at height 174 m.a.s marked by purple colour-bar over model-terrain, equal to as presented in (Fig. 2). The direction of the wind in the model is illustrated by arrows. The representation of the conditions depicted illustrates the specific conditions during the icing event at which the ice accretion rate is at its peak, 13:00 on the 20th of January.

For the represented geographical area there is a clear wind direction coming from NW. This evidently force winds to follow the fjord in direction toward the site of interest, marked in red ellipse. Identifying areas with high LWC there seems to be a prominent relation to higher LWC located over higher terrain elevation that is first faced by the winds.

Fig. 7 shows a vertical cross section with stating point in the green dot following the line to the end point in the red dot marked in (Fig. 6).

The wind direction is parallel to the line, meaning that the direction of the wind in (Fig. 7) flows directly from left to right relative to the figure. In the figure the white dashed lines represent temperature $[°C]$, purple lines RH [%], and the colour-bar LWC [kg/kg]. The model terrain is illustrated by the brown filled sections. The total length of the cross section is 40 km where the site is located 1 km before the highest peak.

Orographic lifting due to winds forcing air to follow the terrain will cool the air and condensation of water vapour will increase the LWC. The figure shows how LWC is consequently increasing with its maximum value located at and around the top of the mountain. The site located near the top at the windward side will experience a higher LWC compared to surrounding areas during north-westerly winds.

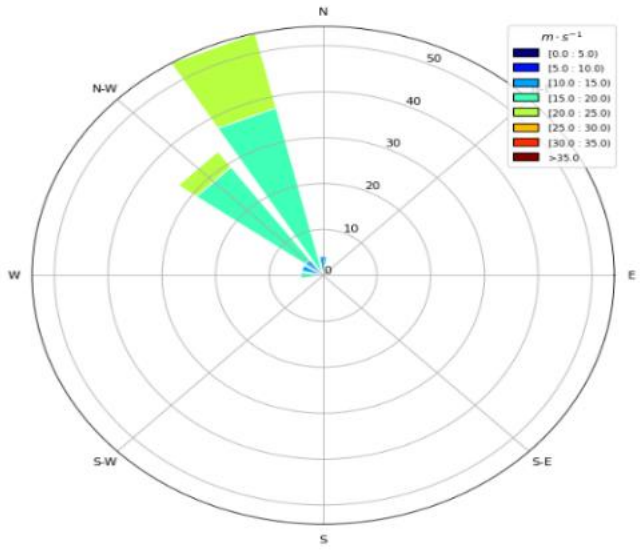

Fig. 5 Wind rose for hourly averaged values at times where icing intensity exceeds 0 g/h at height 174 m.a.s.

Orographic lifting might be the most significant reason for a relatively high LWC observed at the site when seen in relation to relatively low temperatures.

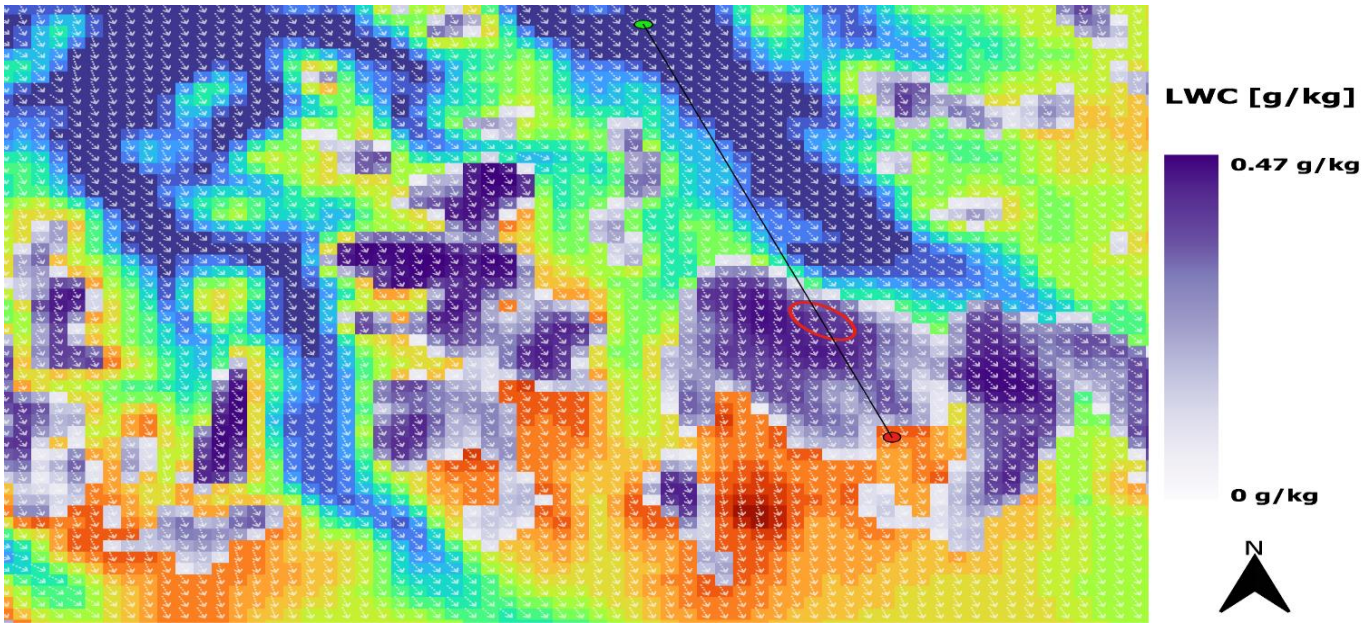

Fig. 6 Overview of the LWC from layer 174 m.a.s over model terrain extracted from model domain 3 at timestamp 13:00 on the 20.01.2022. The direction of the wind at the same layer-height for each grid cell is marked by the arrows. The green dot marks the starting point and the red dot the ending point for the vertical cross-section shown in Fig. 7. The red ellipse illustrated the approximate location of the suggested site.

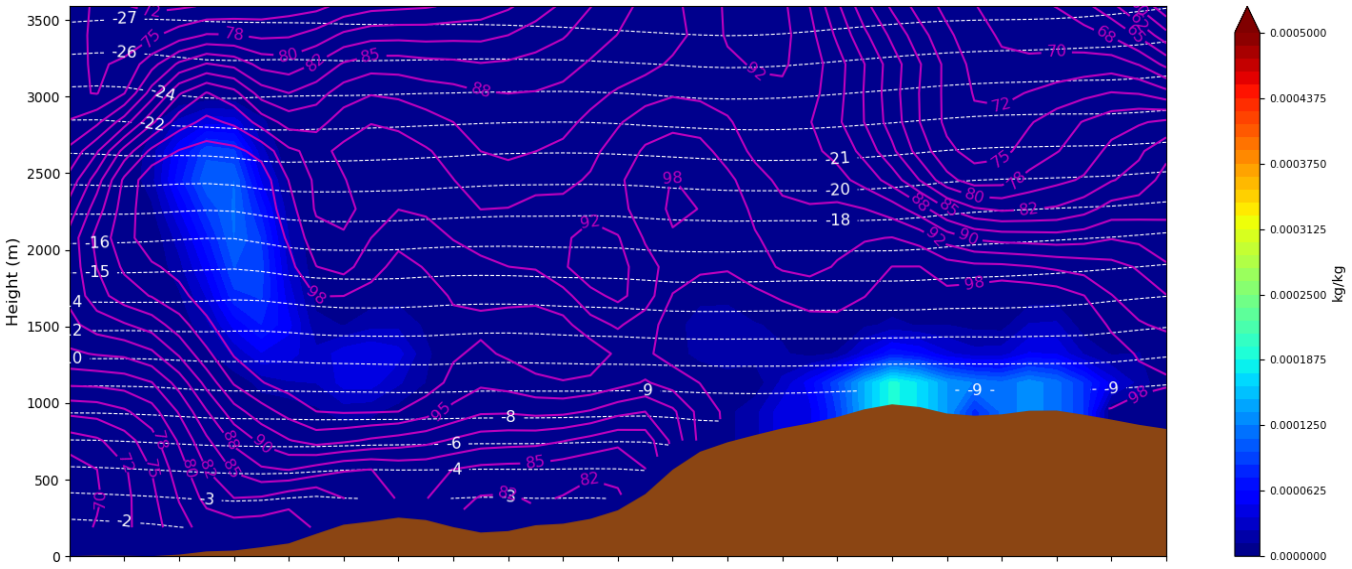

Fig. 7 Vertical cross-section with horizontal length 40km with start and end point as illustrated in Figure 4.29. The models vertical height is represented in meters above sea level and model terrain is marked in brown. The vertical cross-section shows temperature [**°C**] (white),relative humidity [%] (purple) and LWC [kg/kg] (colour-bar).

IV. Conclusions

There are no available measurements from the proposed site, and the analysis used output data from the NWP model WRF with a horizontal resolution of 1 km. The time-period considered covered the year of 2022.

The modelled ice accretion shows that the turbine located at the highest terrain elevation has the highest number of yearly icing hours, with 948 hours for icing rates above 10 g/h. The turbine located at lowest elevation has the lowest number of total annual hours, with 385 hours for icing rates exceeding 10 g/h. This shows large deviations in estimated icing intensity within the site. Model terrain elevation is found to be strongly connected to the ice accretion rate. Because of this, a method for adjusting the icing estimations to differences between model and actual terrain height is conducted. This aims to provide more accurate results.

Analysis of wind patterns at times with meteorological icing, shows that ice accretion normally accumulates during winds coming from north-westerly directions. The case studies shows that icing conditions with north-westerly winds induce an increased LWC because of orographic lifting. This is the main cause for ice accretion at the site.

Acknowledgment

The authors wish to thank Troms Kraft for their collaboration.

References

[1] Hochart, C., et al., *Wind turbine performance under icing conditions.* Wind Energy: An International Journal for Progress and Applications in Wind Power Conversion Technology, 2008. 11(4): p. 319-333.

[2] Homola, M.C., *Atmospheric icing on wind turbines: Modeling and consequences for energy production.* 2011

[3] Seifert, H., *Technical requirements for rotor blades operating in cold climate.* DEWI-Magazin, 2005

[4] Contreras Montoya, L.T., S. Lain, and A. Ilinca, *A review on the estimation of power loss due to icing in wind turbines.* Energies, 2022. 15(3): p. 1083

[5] Ebrahimi, A., *Atmospheric icing effects of S816 airfoil on a 600 kW wind turbine's performance.* Scientia Iranica, 2018. 25(5): p. 2693-2705

[6] Homola, M.C., et al., *Performance losses due to ice accretion for a 5 MW wind turbine.* Wind Energy, 2012. 15(3): p. 379-389

[7] Thorsson, P., S. Söderberg, and H. Bergström, *Modelling atmospheric icing: A comparison between icing calculated with measured meteorological data and NWP data.* Cold regions science and technology, 2015. 119: p. 124-131

[8] W. C. Skamarock, J. B. Klemp, J. Dudhia, D. O. Gill, Z. B. J. Liu and X. Y. Huang, *A description of the advanced research WRF model version 4.*, Atmospheric Research, 2019.

[9] H. Hersbach, *The ERA5 Atmospheric Reanalysis*, in AGUFM, NG33D-01., 2016

[10] Thompson, G., et al., *Explicit forecasts of winter precipitation using an improved bulk microphysics scheme. Part II: Implementation of a new snow parameterization.* Monthly weather review, 2008. 136(12): p. 5095-5115

[11] Dudhia, J., *WRF physics options.* NCAR WRF basic tutorial, 2010. 26: p. 30

[12] Iacono, M.J., et al., *Radiative forcing by long-lived greenhouse gases: Calculations with the AER radiative transfer models.* Journal of Geophysical Research: Atmospheres, 2008. 113(D13

[13] Mukul Tewari, N., et al. *Implementation and verification of the unified NOAH land surface model in the WRF model (Formerly Paper Number 17.5).* in *Proceedings of the 20th conference on weather analysis and forecasting/16th conference on numerical weather prediction*, Seattle, WA, USA. 2004

[14] ISO 12494, *Atmospheric icing of structures, first edition*, 2001

[15] Thompson, G., Nygaard, B. E., Makkonen, L., & Dierer, S. (2009). *Using the Weather Research and Forecasting (WRF) model to predict ground/structural icing*. 13th International Workshop on Atmospheric Icing on Structures, METEOTEST, Andermatt, Switzerland

[16] Hämäläinen, K. and S. Niemelä, *Production of a numerical icing atlas for Finland.* Wind Energy, 2017. 20(1): p. 171-189

[17] Strand, J.M, *Atmospheric in-cloud icing using WRF for an alpine wind power plant in Kvænangen*, Master's thesis, University of Tromsø – The Arctic University of Norway, 2023